Polymer Deconstructability and Recyclability
***via* Introduction of Cleavable Si−O Bonds**

By
Alayna Johnson
Bachelor of Science in Chemistry
University of Illinois at Urbana Champaign, 2020

SUBMITTED TO THE DEPARTMENT OF CHEMISTRY IN PARTIAL FULFILLMENT OF THE REQUIREMENTS FOR THE DEGREE OF

MASTER OF SCIENCE IN CHEMISTRY
AT THE
MASSACHUSETTS INSTITUTE OF TECHNOLOGY

February 2025

Authored by:

Alayna Johnson
Department of Chemistry
January 17, 2025

Certified by:

Adam P. Willard
Professor of Chemistry
Thesis Supervisor

Accepted by:

Adam P. Willard
Professor of Chemistry
Graduate Officer

Polymer Deconstructability and Recyclability
***via* Introduction of Cleavable Si−O Bonds**

By

Alayna Johnson

Submitted to the Department of Chemistry
on January 17, 2025 in Partial Fulfillment of the
Requirements for the Degree of
Master of Science in Chemistry

ABSTRACT
The synthesis of a new polysilylether *via* entropy-driven ring-opening metathesis polymerization (ED-ROMP) of cyclic bifunctional silyl ether-based monomers is reported. High molecular weight polymers (up to 100 k) with narrow dispersities were achieved at modest temperature. These polymers display excellent thermal stability and ultra-low T_g (–88 ºC). The polymers are both rapidly deconstructable *via* the cleavage of the labile silicon-oxygen linkages with either acid or fluoride triggers and partially depolymerizable by the addition of exogenous metathesis catalyst. Analysis of the deconstructed polymer products provided insight into the polymer microstructure, showing that the ED-ROMP process was regiorandom. Altogether, this work offers a new class of deconstructable polymers with a range of potential applications. Incorporation of these bifunctional silyl ether-based monomers into copolymers could aid in the triggered deconstruction of otherwise nondegradable hydrocarbon backbones.

Thesis Supervisor: Adam P. Willard
Title: Professor of Chemistry

The thesis has been transcribed from the below article written by the author:

Johnson, A. M., Husted, K. E. L., Kilgallon, L. J., & Johnson, J. A. (2022). Orthogonally Deconstructable and Depolymerizable Polysilylethers. *Chemical Communications*, *58*(61), 8496–8499. doi: 10.1039/d2cc02718f.

TABLE OF CONTENTS **Pg.**

LIST OF FIGURES, TABLES, AND SCHEMES **Pg.**

INTRODUCTION

Synthetic polymer production has increased exponentially over the past 50 years, due in large part to their numerous applications ranging from industrial goods to consumer products and medical equipment.[1] However, in the absence of efficient deconstruction methods, most widely used plastics persist in the environment for centuries beyond their functional lifetime. In some cases, the polymer properties that make attractive consumer and industrial goods (*e.g.*, high strength and low density) are the very aspects that make deconstructability challenging.[2] For example, although synthetic polymers comprise only approximately 11% of the total municipal solid waste (MSW) stream by mass, they occupy a disproportionate volume in landfills due to their low density.[3] Unlike other components of the MSW stream, most synthetic polymers are not biodegradable and can remain in landfills indefinitely.[4] 80 million tons of plastic are produced annually for packaging alone. Of this, more than 40% is discarded into landfills after just a single use and 32% escapes conventional collection streams, often becoming ocean pollutants.[5] Although plastic comprises a relatively small portion of the MSW, more than 80% of marine pollutants are plastic, and experts predict that plastic ocean pollutants will outweigh the mass of fish by 2050.[5]

Thus, there is continued interest in developing chemically labile bonds that facilitate the deconstruction of plastics, as well as in exploring the processes used to synthesize these materials. Ring-opening metathesis polymerization (ROMP) is a powerful tool for the synthesis of linear polymers with controlled size, architecture, and thermomechanical properties. Following reports of olefin metathesis for polymer synthesis in the 1960s using heterogeneous mixtures of transition-metal halides, ruthenium, and molybdenum-based catalysts were introduced by Grubbs and Schrock in the 1990s and ushered in a new era of highly active metathesis catalysts (**Figure 1a).**[6,7,8]

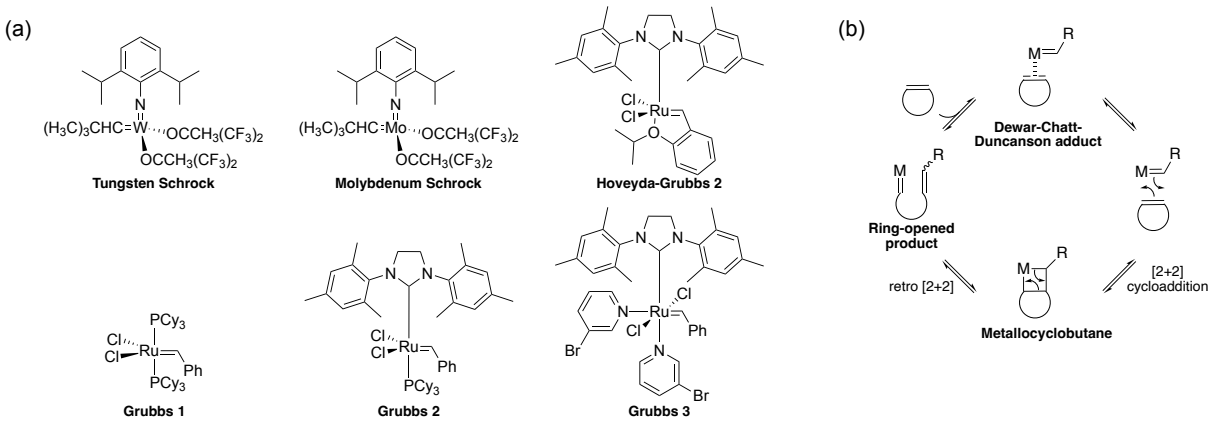

Figure 1. (a) Tungsten, molybdenum, and ruthenium catalysts used for ROMP.[9] (b) General ring-opening metathesis polymerization (ROMP) mechanism.[8]

The general mechanism for ROMP begins with the coordination of a cyclic alkene monomer to the metal alkylidene catalyst, followed by a [2 + 2] cycloaddition to give a stable metallacyclobutane intermediate.[8] A retro [2 + 2] mechanism opens the cyclic olefin and forms a new metal alkylidene active center (**Figure 1b**).[8]

The ability of a monomer to readily undergo ROMP is dependent on the free enthalpy (ΔH_p) and entropy (ΔS_p) of polymerization as well as the equilibrium monomer concentration ($[M]_{eq}$) as expressed in Equation 1.[10]

$$\ln[M]_{eq} = \frac{\Delta H_p}{RT} - \frac{\Delta S_p}{R} \quad (1)$$

In most polymerizations of small (three- to six- membered) cyclic monomers, the reaction driving force is alleviation of ring strain and associated decrease in enthalpy upon ring-opening, which compensates for the accompanied decrease in translational entropy of the growing polymer chain.[11] For somewhat larger (five- to eight- membered) cyclic olefins, alleviation of angular and transannular strain provides a moderate enthalpic driving force for polymerization. In these cases, the favorable enthalpic contribution and the unfavorable entropic contributions can be nearly equal and $[M]_{eq}$ becomes higher.[12]

During polymerization of moderately-strained monomers, macrocycles can arise by either end-to-end ring closure or by backbiting reactions.[13] This process can be predicted according to the theory of Jacobson and Stockmayer.[14] This describes the $[M]_{eq}$ for a macrocycle of γ repeat units and suggests that this equilibrium concentration will decrease as the ring-size increases according to Equation (2).

$$[M(\gamma)]_{eq} \sim \gamma^{-5/2} \quad (2)$$

Subsequent modeling by Kornfield and coworkers indicates that ring strain also contributes to the critical monomer concentration.[15] Together, these theories describe how the distribution of cyclic and linear species at equilibrium has significant dependence on monomer concentration. The relative magnitudes of the enthalpic and entropic terms of polymerization will determine the direction of temperature control. Reaction conditions can be altered to control ring-chain equilibrium and to favor polymerization of moderate-strain monomers. For example, since cyclization is a unimolecular process and polymerization is a bimolecular process, equilibrium favors intramolecular cyclization under dilute conditions and intermolecular chain polymerization under concentrated conditions. Therefore, high monomer concentration and low reaction temperature can be employed to promote linear chain polymerization.

The driving force behind ROMP is usually release of ring strain, which offsets the entropic costs of with polymerization.[16] However, when rings are large or contain especially flexible bonds, atoms can achieve near-ideal bond angles, so the enthalpic benefit of polymerization

becomes negligible. Consequently, the reaction will yield a distribution of monomers, oligomers, and polymer chains at equilibrium.[15] These reactions can be biased towards polymerization if the polymer repeat unit exhibits a greater number of rotational and vibrational microstates than the monomer—a process known as entropy-controlled ring-opening metathesis polymerization (ED-ROMP).[17] Grubbs and coworkers documented the first studies of modern ED-ROMP with crown ethers in 1997.[18] More recent examples include ED-ROMP of cyclic olefins equipped with ester and disulfide functionalization.[19,20]

Thus, ED-ROMP is a promising route for the introduction of interesting backbone chemistries.[21] Given the global plastic waste crises, the introduction of degradable and/or bioderived moieties into otherwise recalcitrant hydrocarbon polymers is especially relevant. For example, Hillmyer and coworkers recently studied high-molecular weight bio-based poly(ricinoleic acid) synthesized *via* ED-ROMP.[22] This report utilizes these principles to install silyl ether (Si–O) bonds into deconstructable polymers. Silyl ethers are an attractive choice for this application because they not only have an unusually high bond strength (Si–O ~108 kcal mol^{-1}) but are also easily deconstructable with a variety of chemical triggers. [23,24]

Johnson and coworkers previously studied 8-membered cyclic silyl ether olefins and found that they could be efficiently prepared and statistically copolymerized with a variety of ROMP-active norbornene derivatives, giving way to applications in recyclable thermosets and drug delivery.[23,25,26] However, at the concentrations at which these copolymerizations were previously conducted (50 mM), no homopolymerization was observed.[23] Stemming from this observation, this study sought to identify conditions under which these monomers could be homopolymerized, as it is anticipated that their respective polymers could possess desirable properties including polydimethylsiloxane-like thermal properties and facile deconstructability.[27]

RESULTS AND DISCUSSION

POLYMER SYNTHESIS VIA ED-ROMP

To begin the investigation, an eight-membered bifunctional silyl ether olefin (^{i}PrSi8) was treated with 0.002 equivalents (with a total target number-average degree of polymerization (DP) of 500) of third-generation Grubbs bispyridyl complex (G3) for two hours (**Scheme 1**). Initial screening was performed at $[M]_0$ = 500 mM and the reaction was quenched after 2 h by adding excess ethyl vinyl ether.

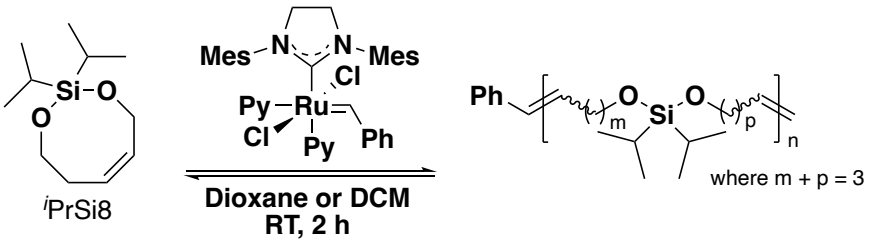

Scheme 1. Homopolymerization of eight-membered ^{i}PrSi8 via ROMP.

SEC analysis of the ^{i}PrSi8 homopolymerization reaction mixture revealed high molecular weight species, consistent with successful ROMP. Therefore, a variety of temperatures were screened to optimize the reaction conditions (**Scheme 1**, **Table 1** entries 1-5). Initial screening covered a range of low temperatures (–78ºC to 3ºC) because performing conventional enthalpy-controlled ROMP at low temperatures can mitigate the entropic penalty of polymerization and drive the reaction toward high-molecular weight polymer.[15] Instead, however, higher conversion and number-average molar mass (51.2% conversion, M_n = 47.7 kDa at 3 °C) were observed at higher temperatures, indicative of ED-ROMP.[13] Attempts to polymerize ^{i}PrSi8 at higher temperatures (35ºC to 60ºC) yielded an isomerization feature at 6.4 ppm by ^{1}H NMR, which grows as the reaction temperature increases (**Figure 2a**).

Table 1. ROMP of ^{i}PrSi8 at Varying Temperatures and Kinetics of ^{i}PrSi8 Homopolymerization[a]

entry	T (ºC)	time (min)	conv. (%)[b]	$M_{n,theo}$ (kDa)[c]	$M_{n,SEC}$ (kDa)[d]	$Đ^{d}$
1	-78	120	28.8	31.0	36.5	1.94
2	-18	120	46.7	50.1	41.9	1.50
3	-10	120	47.8	51.2	43.8	1.97
4	0	120	50.7	54.3	46.8	1.63
5	3	120	51.2	55.0	47.7	1.61
6	RT	0.25	7.5	16.1	3.5	1.10
7	RT	0.5	14.4	30.9	6.0	1.12
8	RT	1	23.3	50.2	9.1	1.18
9	RT	2	38.3	82.1	15.1	1.26
10	RT	5	63.6	136	22.8	1.53
11	RT	60	95.4	204	136	1.70
12	RT	120	96.1	206	159	1.76

[a]ROMP was performed in DCM (low T) or dioxane (high T) under N_2 and quenched with ethyl vinyl ether. A feed ratio of 500:1 $[M]_0$:[G3] and a monomer concentration of $[^{i}PrSi8]_0$=500 mM were used for all reactions. [b]Monomer conversion was determined ^{1}H NMR spectroscopy. [c]Theoretical number-average molar mass $M_{n,theo} = DP_{monomer}$ x $MW_{monomer}$ where DP = feed ratio x conversion. [d]Molar mass and dispersity were determined by size-exclusion chromatography in $CHCl_3$ relative to low dispersity polystyrene standards.

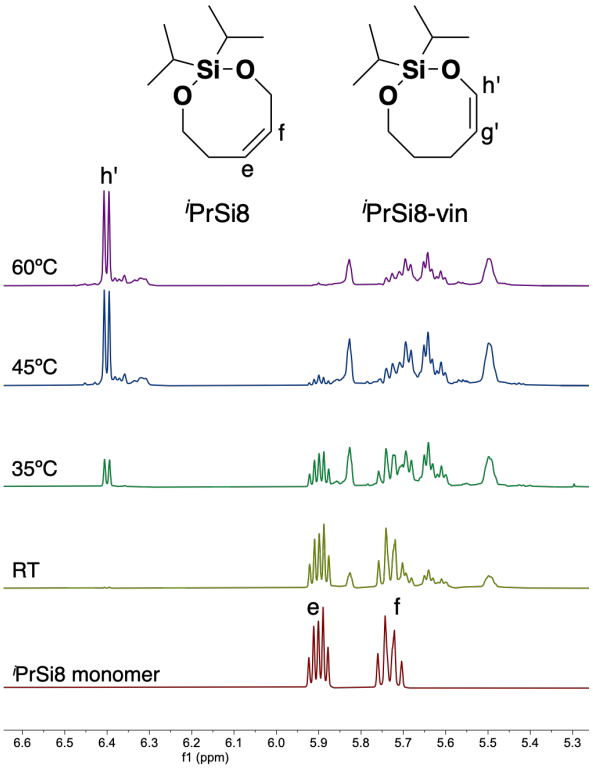

Figure 2. ^{1}H NMR spectra (400 MHz, $CDCl_3$) of olefin region during ROMP of ^{i}PrSi8 at increasing temperature.

Next, simultaneous homopolymerization reactions were set up at room temperature and quenched at different times (**Table 1** entries 6-10). The polymer number-average molar mass as measured by size-exclusion chromatography ($M_{n,SEC}$) increased linearly as a function of monomer conversion while maintaining low dispersity (1.10-1.53), suggesting a controlled polymerization (**Figure 3a**). Using the method of initial rates, plotting $\ln([M]/[M]_0)$ as a function of time revealed a linear relationship to 5 min, consistent with pseudo-first order kinetics (**Figures 3b-c**).

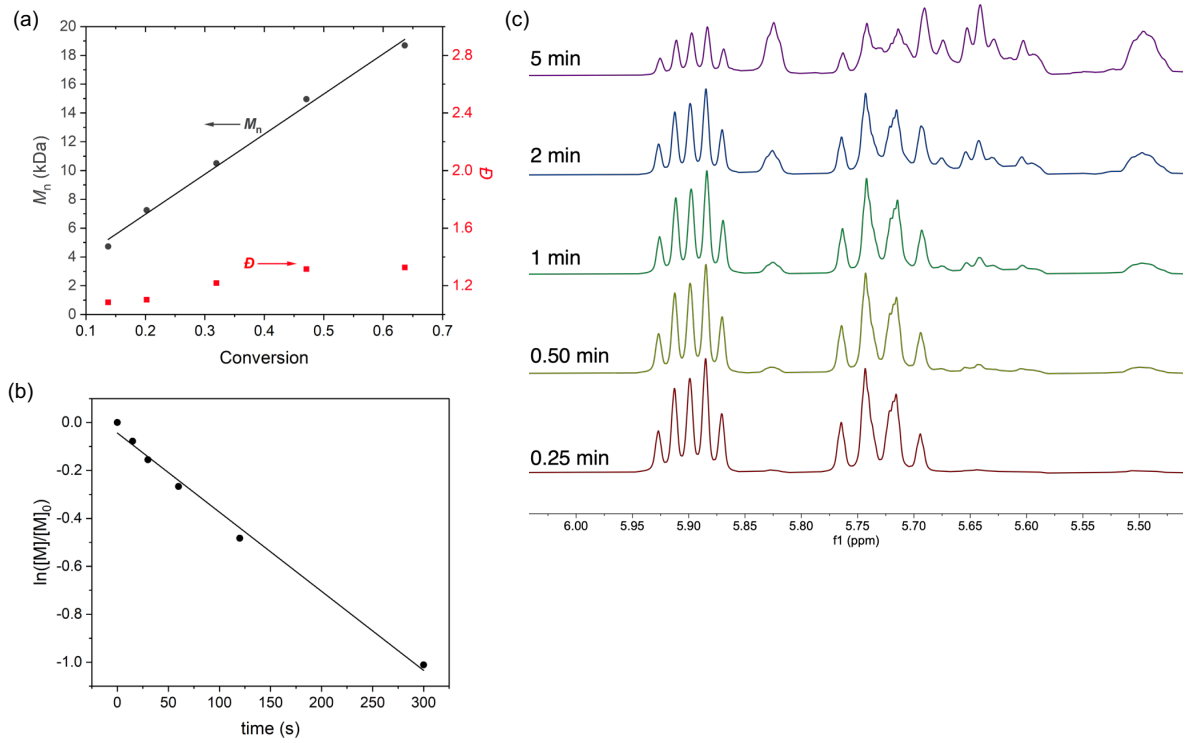

Figure 3. Homopolymerization kinetics were determined following adaptations of previously reported procedures.[28,29] (a) Plot of M_n and $Đ$ vs monomer conversion, obtained by a combination of SEC and ^{1}H NMR analysis. (b) Plot of $\ln([M]/[M]_0)$ as a function of time with $R^2 = 0.992$. (c) ^{1}H NMR spectra (400 MHz, $CDCl_3$) of olefin region during ROMP of ^{i}PrSi8 using 0.002 equivalents of G3.

Allowing the polymerization to proceed for 1 h produced high $M_{n,SEC}$ species (136 kDa) and at 2 h, negligible changes to conversion and M_n were observed, suggesting that the reaction had reached equilibrium between monomer and polymer (**Table 1** entries 11-12). Low molecular weight features were consistently present in the SEC traces of the unpurified polymers (**Figure 4a**), which suggests the formation of cyclic oligomers by backbiting, a common side reaction in ED-ROMP.[22] This behavior is further reflected in a significant difference between the theoretical number-average molar mass ($M_{n,theo}$) and $M_{n,SEC}$ (**Table 1**). It was hypothesized that oligomer formation could be suppressed by increasing the monomer concentration.[22] Thus, polymerizations were carried out at increasing concentration for several hours to ensure sufficient time to reach equilibrium (**Figure 4b**, Table 2 entries 1-5). The relative concentration of cyclic oligomer was estimated by SEC using an RI detector, assuming an equivalent molar RI response. Consistent with expectation, higher concentrations afforded higher molar masses and lower oligomer content; however, a modest increase in dispersity was observed.

Precipitation of the quenched reaction into methanol yielded high molecular weight homopolymer ($M_{n,SEC}$ = 87 kDa, $Đ$ = 1.78) and reduced the cyclic oligomer content below 6%.

Table 2. ROMP of ^{i}PrSi8 at Varying Concentrations and Monomer-to-Catalyst Ratios[a]

entry	$[M]_0/[\mathbf{G3}]^b$	Conc. (M)[c]	$M_{n,SEC}$ (kDa)[d]	$Đ$[d]	Cyclic Oligomer Content (%)[e]
1	500	0.05	0.42	1.02	100
2	500	0.50	57.7	1.42	68
3	500	1.0	135	1.76	27
4	500	2.0	156	1.86	21
5	500	2.0[e]	87	1.78	5.6
6	50	2.0	22.4	1.52	–
7	100	2.0	44.1	1.49	–
8	500	2.0	138	1.53	–
9	1000	2.0	183	1.68	–

[a]ROMP was performed in dioxane under N_2 for 2 h at RT and quenched with ethyl vinyl ether. [b]Feed ratio of monomer to G3. [c]Initial monomer concentration. [d]$M_{n,SEC}$ and $Đ$ were determined by SEC in $CHCl_3$ relative to low $Đ$ polystyrene standards. [e]Calculated from the area percentage of RI chromatographs of SEC.

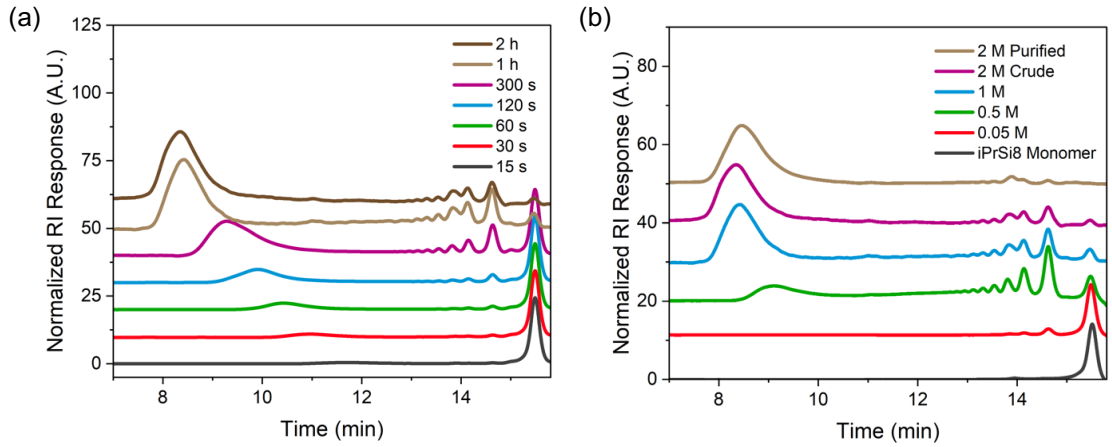

Figure 4. (a) SEC traces (normalized RI) of **poly(^{i}PrSi8)** quenched at different reaction times (correlated to **Table 1**, entries 6-12). (b) SEC traces of **poly(^{i}PrSi8)** prepared at increasing monomer concentration in dioxane (correlated to **Table 2**, entries 1-5).

ORTHOGONAL DECONSTRUCTION AND DEPOLYMERIZATION

Since ED-ROMP reactions lack a significant enthalpic driving force, the polymerization exists in an equilibrium of rings and chains.[30] To capitalize on this ring-chain equilibrium for depolymerization, depolymerization was probed by preparing a stock solution of poly(^{i}PrSi8) (**Table 2** entry 2), collecting aliquots, and exposing each to different amounts of G3. SEC traces of each depolymerization reaction compared to a reference sample that was not treated with additional G3 demonstrate that the size of the polymer chain can be reduced by an order of magnitude (from 58 kDa to 5.5 kDa) under these conditions (**Figure 5a**). ^{1}H NMR spectra of

the G3-treated mixture indicate that the depolymerization mechanism leads to the reformation of ^{i}PrSi8 monomer in ~28% yield (**Figure 5b**). A similar result was observed for larger homopolymers; treatment of DP 1000 poly(^{i}PrSi8) (**Table 2** entry 9) with 5 eq G3 reduced its molar mass from 183 to 16.8 kDa (**Figure 5c**).

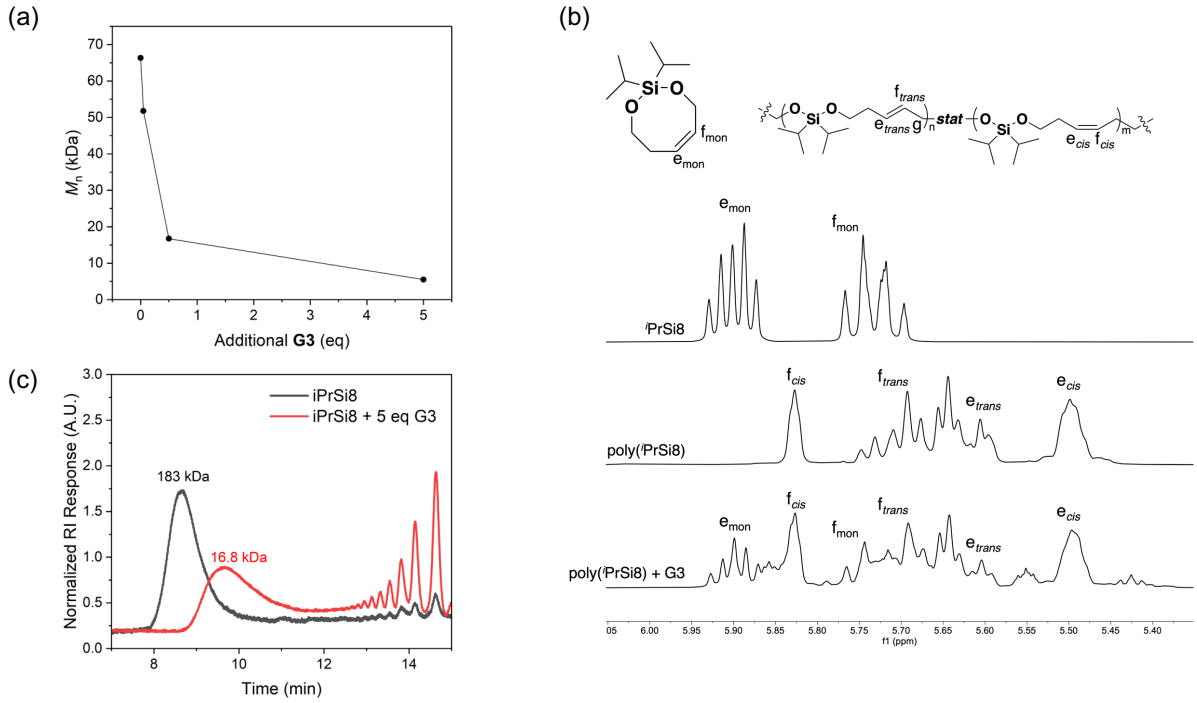

Figure 5. (a) Polymer size (obtained by SEC) of homopolymer prepared from 500 mM ^{i}PrSi8 (**Table 2** entry 2) as it is exposed to increasing amounts of additional G3. (b) ^{1}H NMR spectra (400 MHz, $CDCl_3$) of olefin region of ^{i}PrSi8, poly(^{i}PrSi8), and poly(^{i}PrSi8) treated with 5 x 10^{-4} mmol additional G3 initiator. The yield of reformed monomer was estimated by integrating the e_{mon} features in the depolymerized spectrum. (c) SEC traces of crude DP 1000 poly(^{i}PrSi8) (gray) and DP 1000 poly(^{i}PrSi8) treated with 0.0035 mmol additional G3 (red). A molar mass decrease from 183 kDa to 16.8 kDa is observed upon depolymerization.

As noted above, silyl ethers represent robust yet selectively cleavable functional groups that can be exploited for polymer backbone deconstruction;[23] thus, it was hypothesized that poly(^{i}PrSi8) could be chemically deconstructed orthogonally to depolymerization. Samples of poly(^{i}PrSi8) of various DP were synthesized and subjected to deconstruction conditions (**Table 2** entries 6-9). Given the well-established precedent of cleaving Si-O bonds with Brønsted acids and fluoride ions, each polymer was separately exposed to 0.5 M HCl in dioxane or 0.2 M tetrabutylammonium fluoride (TBAF, **Figure 6a**, step *i*) in THF at room temperature for fifteen minutes (Figure S17, S19).[23,25] Under both conditions, no high molecular weight species were detected by SEC (**Figure 6b**), suggesting complete backbone deconstruction. It is thought that by modifying the steric bulk and polarity of the silyl substituents, different backbone deconstruction rates could be achieved.[23,31]

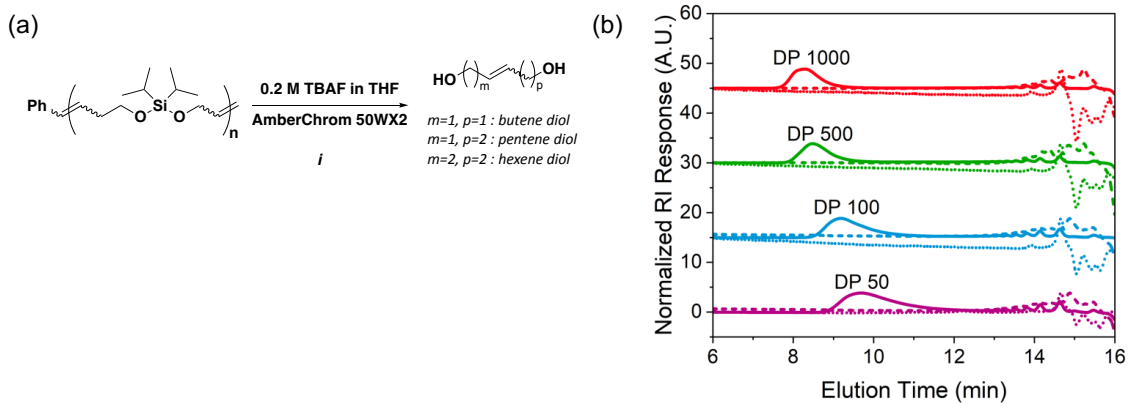

Figure 6. (a) Fluoride-triggered deconstruction of poly(*i*PrSi8). (b) SEC traces (normalized RI) of poly(*i*PrSi8) to different target DP (solid line, correlated to **Table 2** entries 6-9) and subsequent deconstruction with 0.2 M TBAF in THF (dotted line) and 0.5 M HCl in dioxane (dashed line).

DETERMINATION OF REGIOSELECTIVITYELECTIVITY

ED-ROMP reactions are known to involve intra- and inter-metathesis mechanisms that can alter the regio- and stereo- chemistry of the growing polymer chain.[22] While it is possible to use methods like ^{1}H NMR to characterize homopolymer regio- and stereo-regularity, as was done by Hillmyer and coworkers to determine that the ED-ROMP of ricinoleic acid forms a regiorandom polymer, new methods for the characterization of the microstructure of backbone degradable polymers are of interest. The fluoride-mediated deconstruction of poly(*i*PrSi8) yields a mixture of isolable diols, the composition of which should encode information about the polymer microstructure (**Figure 7a**). Thus, a gas-chromatography mass-spectrometry (GC-MS) assay was designed to characterize the deconstructed product mixture. Initial analysis of the fluoride-deconstructed mixture via GC-MS showed six distinct features: *cis* and *trans* isomers of butene, pentene, and hexene diols, which correspond to head-to-head (HH), head-to-tail or tail-to-head (HT/TH), and tail-to-tail (TT) polymer segments, respectively (**Figure 7b**).

Unfortunately, due to the chemically similar nature of the *cis* and *trans* diol derivatives, complete resolution of this mixture was not possible. Initial attempts to hydrogenate the unprotected diol mixture and simplify analysis were unsuccessful; hydrogenation of small unsaturated diols is known to form several side products, which would bias the product ratio.[32] This obstacle was circumvented by acetylating the unsaturated diol mixture (**Figure 7a**, step *ii,* Figure S20-21) and then hydrogenating to yield a mixture of 1,4-diacetoxybutane, 1,5-diacetoxypentane and 1,6-diacetoxyhexane in quantitative yield (**Figure 7a**, step *iii,* Figure S22-23). Aliphatic acetylated calibration standards were prepared and measured separately (Figure S24-S25). Using this method, the ratio of HH : HT/TH : TT ratio was found to be 1 : 2 : 1 (**Figure 7c**, Table S1). This observation strongly suggests that the homopolymerization is regiorandom, as a regioregular polymerization would lead to preferential formation of 1,5-diacetoxypentane under these conditions (**Figure 7d**).

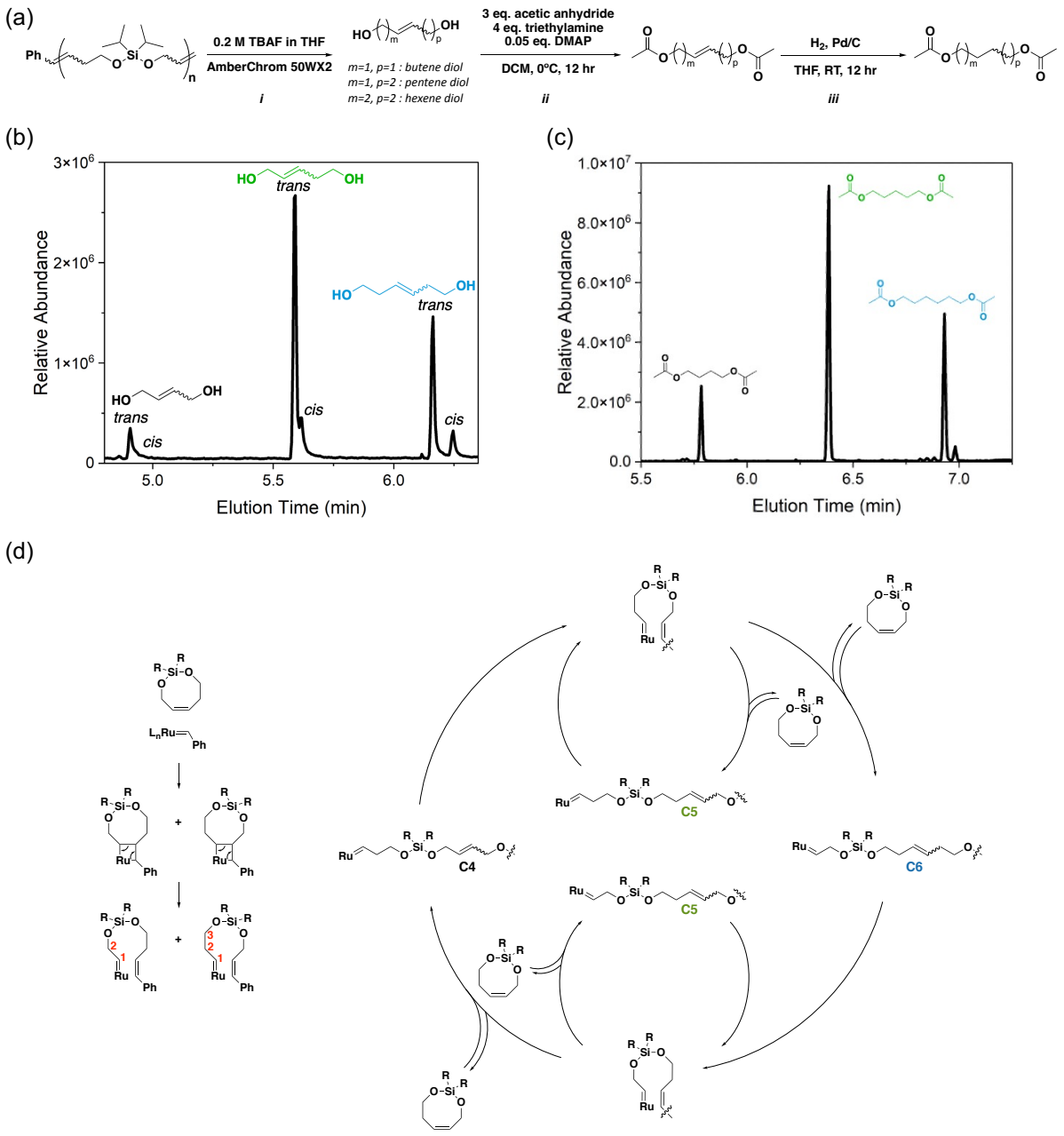

Figure 7. (a) Fluoride-triggered deconstruction (*i*), acetylation (*ii*), and hydrogenation (*iii*) of poly(ⁱPrSi8) to yield a mixture of protected saturated diols. (b) GCMS output of fluoride-treated poly(ⁱPrSi8). C4, C5, and C6 regions are easily separable from each other, but *cis*/*trans* isomers are not separable, preventing quantitative analysis. (c) GCMS output of the mixture obtained in **Figure 7a**, which reflects the regiochemical makeup of the original polymer. Comparison to a series of calibration standards reveals a 1:2:1 ratio of the C4, C5, and C6 products, which is consistent with a regiorandom polymer. (d) Proposed mechanism for the formation of 4-, 5-, and 6- carbon segments along the polymer chain.

INVESTIGATION OF THERMAL PROPERTIES

Finally, the thermal properties of poly(*i*PrSi8) were investigated. The purified polymers appeared as light pink viscous oils at room temperature, consistent with a low glass transition temperature (T_g) amorphous material. Thermogravimetric analysis (TGA) revealed high thermal stability of the precipitated poly(*i*PrSi8) under nitrogen. At a heating rate of 20 °C min^{-1}, the fastest rate of mass loss did not occur until 486 ºC as might be expected for siloxane- and olefin-containing polymers (**Figure 8a**). Of note, TGA conducted on the crude polymer before precipitation showed multi-stage mass loss, consistent with the non-degradative loss of volatile low-molecular weight species such as the cyclic oligomers observed in the SEC traces of the crude mixture.

No major thermal transitions, including T_g, were detectable above -75 °C via differential scanning calorimetry (DSC) (**Figure 8b**). This result is consistent with other siloxane-containing polymers such as PDMS, which have glass transition temperatures as low as -123 °C due to the near-zero rotational barrier around O-Si-O bonds.[33] Additionally, poly(*i*PrSi8) contains both *cis* and *trans* olefins in its backbone and a mixture of 4-, 5-, and 6-carbon linkages between silyl ethers; this combination of stereo- and regio-irregularity is likely to render crystallization difficult at temperatures accessible on conventional DSC instruments. Subsequently, ultra-low temperature DSC conditions were pursued to identify a T_g for these materials. A heating rate of 20 °C min^{-1} revealed that a discernible glass transition occurs at -88 °C (**Figure 8c**). Therefore, poly(*i*PrSi8) represents an ultra-low-T_g polymer that is also highly resistant to crystallization, potentially facilitating applications in low-temperature environments.

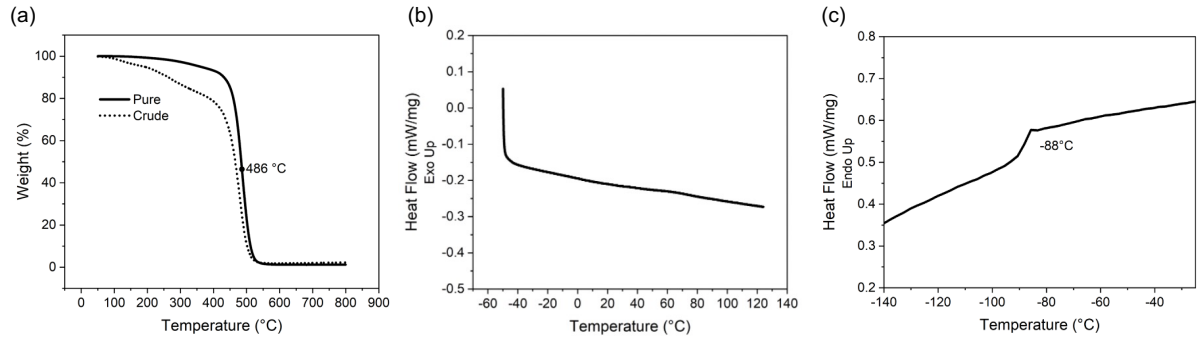

Figure 8. Thermal characterization of poly(*i*PrSi8) (DP = 1000). **(a)** Thermogravimetric analysis of crude homopolymer (dotted line) and purified polymer (solid line) under nitrogen atmosphere with a heating rate of 20 °C/min. The first derivative of the weight % reaches a minimum at 486 ºC. (b) Differential scanning calorimetry traces of poly(*i*PrSi8) showing no T_g above -78 ºC. (c) Differential scanning calorimetry thermogram. The third heating scan under nitrogen at a heating rate of 10 °C/min reveals a glass transition temperature of -88 °C.

CONCLUSION

In conclusion, novel polysilylether homopolymers were synthesized by ED-ROMP, analyzed, and subsequently deconstructed. The ED-ROMP of an eight-membered cyclic silyl ether olefin produced a high molecular weight polymer with an extremely low glass transition temperature (T_g) of –88ºC. These materials demonstrated rapid backbone deconstructed when treated with both acid and fluoride and partial depolymerization when treated with G3. Future research may explore the copolymerization of silyl ether monomers with olefins that are active in ROMP to create deconstructable hydrocarbon-based polymers.

REFERENCES

(1) Trucost. Natural Capital at Risk: The Top 100 Externalities of Business. *Teeb* **2013**, No. 4, 1–43.

(2) Schneiderman, D. K.; Hillmyer, M. A. 50th Anniversary Perspective: There Is a Great Future in Sustainable Polymers. *Macromolecules* **2017**, *50*, 3733–3749.

(3) Themelis, N. J.; Mussche, C. 2014 Energy and Economic Value of Municipal Solid Waste (MSW), Including Non-Recycled Plastics (NRP), Currently Landfilled in the Fifty States. *Columbia Univ.* **2014**, 40.

(4) Raynaud, J. *Valuing Plastics: The Business Case for Measuring, Managing and Disclosing Plastic Use in the Consumer Goods Industry*; 2014.

(5) Gravis, L. The New Plastics Economy: Rethinking the Future of Plastics & Catalysing Action. *Ellen MacArthur Found.* **2017**, 68.

(6) Natta, G.; Dall'Asta, G.; Bassi, I. W.; Carella, G. Stereospecific Ring Cleavage Homopolymerization of Cycloolefins and Structural Examination of the Resulting Homologous Series of Linear Crystalline Trans Polyalkenamers. *Die Makromol. Chemie* **1966**, *91*, 87–106.

(7) Schrock, R. R.; Hoveyda, A. H. Molybdenum and Tungsten Imido Alkylidene Complexes as Efficient Olefin-Metathesis Catalysts. *Angew. Chem. Int. Ed.* **2003**, *42*, 4592–4633.

(8) Trnka, T. M.; Grubbs, R. H. The Development of L2X2RU=CHR Olefin Metathesis Catalysts: An Organometallic Success Story. *Acc. Chem. Res.* **2001**, *34*, 18–29.

(9) Martinez, H.; Ren, N.; Matta, M. E.; Hillmyer, M. A. Ring-Opening Metathesis Polymerization of 8-Membered Cyclic Olefins. *Polym. Chem.* **2014**, *5*, 3507–3532.

(10) Duda, A.; Kowalski, A. *Thermodynamics and Kinetics of Ring - Opening Polymerization*; Philippe, D., Olivier, C., Raquez, J.-M., Eds.; WILEY-VCH, 2009.

(11) Hillmyer, M. A.; Laredo, W. R.; Grubbs, R. H. Ring-Opening Metathesis Polymerization of Functionalized Cyclooctenes by a Ruthenium-Based Metathesis Catalyst. *Macromolecules* **1995**, *28*, 6311–6316.

(12) Walker, R.; Conrad, R. M.; Grubbs, R. H. The Living ROMP of Trans-Cyclooctene. *Macromolecules* **2009**, *42*, 599–605.

(13) Pearce, A. K.; Foster, J. C.; O'Reilly, R. K. Recent Developments in Entropy-Driven Ring-Opening Metathesis Polymerization: Mechanistic Considerations, Unique Functionality, and Sequence Control. *Journal of Polymer Science, Part A: Polymer Chemistry*. 2019, pp 1621–1634.

(14) Kricheldorf, H. R.; Weidner, S. M.; Scheliga, F. Synthesis of Cyclic Polymers and Flaws of the Jacobson-Stockmayer Theory. *Polym. Chem.* **2020**, *11*, 2595–2604.

(15) Chen, Z.; Claverie, J. P.; Grubbs, R. H.; Komfield, J. A. Modeling Ring-Chain Equilibria in Ring-Opening Polymerization of Cycloolefins. *Macromolecules* **1995**, *28*, 2147–2154.

(16) Hlil, A. R.; Balogh, J.; Moncho, S.; Su, H. L.; Tuba, R.; Brothers, E. N.; Al-Hashimi, M.; Bazzi, H. S. Ring Opening Metathesis Polymerization (ROMP) of Five- to Eight-

Membered Cyclic Olefins: Computational, Thermodynamic, and Experimental Approach. *J. Polym. Sci. Part A Polym. Chem.* **2017**, *55*, 3137–3145.
(17) Hodge, P.; Colquhoun, H. M. Recent Work on Entropically-Driven Ring-Opening Polymerizations: Some Potential Applications. *Polym. Adv. Technol.* **2005**, *16*, 84–94.
(18) Marsella, M. J.; Maynard, H. D.; Grubbs, R. H. Template-Directed Ring-Closing Metathesis: Synthesis and Polymerization of Unsaturated Crown Ether Analogs. *Angew. Chemie (International Ed. English)* **1997**, *36*, 1101–1103.
(19) Nowalk, J. A.; Fang, C.; Short, A. L.; Weiss, R. M.; Swisher, J. H.; Liu, P.; Meyer, T. Y. Sequence-Controlled Polymers Through Entropy-Driven Ring-Opening Metathesis Polymerization: Theory, Molecular Weight Control, and Monomer Design. *J. Am. Chem. Soc.* **2019**, *141*, 5741–5752.
(20) Behrendt, F. N.; Hess, A.; Lehmann, M.; Schmidt, B.; Schlaad, H. Polymerization of Cystine-Derived Monomers. *Polym. Chem.* **2019**, *10*, 1636–1641.
(21) Bielawski, C. W.; Grubbs, R. H. Living Ring-Opening Metathesis Polymerization. *Prog. Polym. Sci.* **2007**, *32*, 1–29.
(22) Ogawa, R.; Hillmyer, M. A. High Molar Mass Poly(Ricinoleic Acid): Via Entropy-Driven Ring-Opening Metathesis Polymerization. *Polym. Chem.* **2021**, *12*, 2253–2257.
(23) Shieh, P.; Nguyen, H. V. T.; Johnson, J. A. Tailored Silyl Ether Monomers Enable Backbone-Degradable Polynorbornene-Based Linear, Bottlebrush and Star Copolymers through ROMP. *Nat. Chem.* **2019**, *11*, 1124–1132.
(24) Shieh, P.; Hill, M. R.; Zhang, W.; Kristufek, S. L.; Johnson, J. A. Clip Chemistry: Diverse (Bio)(Macro)Molecular and Material Function through Breaking Covalent Bonds. *Chem. Rev.* **2021**, *121*, 7059–7121.
(25) Shieh, P.; Zhang, W.; Husted, K. E. L.; Kristufek, S. L.; Xiong, B.; Lundberg, D. J.; Lem, J.; Veysset, D.; Sun, Y.; Nelson, K. A.; et al. Cleavable Comonomers Enable Degradable, Recyclable Thermoset Plastics. *Nature* **2020**, *583*, 542–547.
(26) Husted, K. E. L.; Shieh, P.; Lundberg, D. J.; Kristufek, S. L.; Johnson, J. A. Molecularly Designed Additives for Chemically Deconstructable Thermosets without Compromised Thermomechanical Properties. *ACS Macro Lett.* **2021**, *10*, 805–810.
(27) Clarson, S. J.; Dodgson, K.; Semlyen, J. A. Studies of Cyclic and Linear Poly(Dimethylsiloxanes): Glass Transition Temperatures and Crystallization Behavior. *Polymer (Guildf).* **1985**, *26*, 930–934.
(28) B. Chang, A.; Lin, T.-P.; B. Thompson, N.; Luo, S.-X.; L. Liberman-Martin, A.; Chen, H.-Y.; Lee, B.; H. Grubbs, R. Design, Synthesis, and Self-Assembly of Polymers with Tailored Graft Distributions. *J. Am. Chem. Soc.* **2017**, *139*, 17683–17693.
(29) Lin, T.-P.; B. Chang, A.; Chen, H.-Y.; L. Liberman-Martin, A.; M. Bates, C.; J. Voegtle, M.; A. Bauer, C.; H. Grubbs, R. Control of Grafting Density and Distribution in Graft Polymers by Living Ring-Opening Metathesis Copolymerization. *J. Am. Chem. Soc.* **2017**, *139*, 3896–3903.
(30) Strandman, S.; Gautrot, J. E.; Zhu, X. X. Recent Advances in Entropy-Driven Ring-Opening Polymerizations. *Polym. Chem.* **2011**, *2*, 791–799.
(31) Parrott, M. C.; Luft, J. C.; Byrne, J. D.; Fain, J. H.; Napier, M. E.; Desimone, J. M.

Tunable Bifunctional Silyl Ether Cross-Linkers for the Design of Acid-Sensitive Biomaterials. *J. Am. Chem. Soc.* **2010**, *132*, 17928–17932.

(32) Musolino, M. G.; Cutrupi, C. M. S.; Donato, A.; Pietropaolo, D.; Pietropaolo, R. Liquid Phase Hydrogenation of 2-Butyne-1,4-Diol and 2-Butene-1,4-Diol Isomers over Pd Catalysts: Roles of Solvent, Support and Proton on Activity and Products Distribution. *J. Mol. Catal. A Chem.* **2003**, *195*, 147–157.

(33) Bahar, I.; Zuniga, I.; Dodge, R.; Mattice, W. L. Conformational Statistics of Poly(Dimethylsiloxane). 1. Probability Distribution of Rotational Isomers from Molecular Dynamics Simulations. *Macromolecules* **1991**, *24*, 2986–2992.

APPENDIX

MATERIALS AND EXPERIMENTAL METHODS

Materials: All reagents were purchased from commercial suppliers and were used without further purification unless otherwise noted. Polymerizations were conducted in anhydrous Sure/Seal DCM or dioxane (Sigma-Aldrich). Reagents were acquired from commercial vendors, including Sigma-Aldrich, Thermo Fisher Scientific, Acros Organics, and Cambridge Isotope Laboratories.

Nuclear Magnetic Resonance (NMR) Spectroscopy: ^{1}H nuclear magnetic resonance (^{1}H NMR) and ^{13}C nuclear magnetic resonance (^{13}C NMR) spectra were acquired at the MIT Department of Chemistry Instrumentation Facility on a Bruker AVANCE III DRX 400 or Neo 500. Chemical shifts are reported in ppm relative to signals from the NMR solvent: for $CDCl_3$, this corresponds to 7.26 for ^{1}H and 77.0 for ^{13}C spectra.

High Resolution Mass Spectrometry (HRMS): High-resolution mass spectrometry (HRMS) measurements were obtained on JEOL AccuTOF 4G LC-plus equipped with an ionSense DART at the MIT Department of Chemistry Instrumentation Facility.

Size Exclusion Chromatography (SEC): Analytical gel permeation chromatography was performed on a Tosoh EcoSEC HLC-8320 with dual TSKgel SuperH3000 columns and an ethanol-stabilized chloroform mobile phase, with sample concentrations of ~1 mg/mL. Samples were filtered through 0.2 μm PTFE syringe filters before injection into the instrument. Molar mass values were calculated according to linear polystyrene calibration standards.

Thermal Gravimetric Analysis (TGA): TGA studies were performed on ~2-3 mg samples. Analyses were performed on a TGA/DSC 2 STAR System (Mettler-Toledo) equipped with a Gas Controller GC 200 Star System. Studies were performed under a constant stream of nitrogen gas at a temperature ramp of 20 °C/min.

Differential Scanning Calorimetry (DSC): Initial DSC analyses were performed on a TGA/DSC 2 STAR System (Mettler-Toledo) equipped with a RCS1-3277 DSC cell and a DSC1-0107 cooling system. Each sample (~6-8 mg) was sealed in an aluminum pan and subjected to three heating/cooling cycles from -50 °C to 125 °C at a rate of 10 °C/min. Low temperature DSC analyses were performed on a NETZSCH 360° system equipped with 214 Corona Sensor and cooled with liquid nitrogen. Each sample (~6-8 mg) was sealed in an aluminum pan and subjected to three heating/cooling cycles from -160 °C to 220 °C at a rate of 10 °C/min. In both cases, the T_g values were recorded from the second heating ramp using the maximum absolute value of the derivative of heat flow with respect to temperature. DSC traces on the second and third heating cycles were identical for all samples reported.

Gas Chromatography-Mass Spectrometry (GC-MS): GC-MS experiments were performed on Agilent 5977B mass spectrometer detector attached to a 7890B gas chromatograph at the MIT Department of Chemistry Instrumentation Facility.

MONOMER AND POLYMER SYNTHESIS

a. ^{i}PrSi8 synthesis

^{i}PrSi8 was prepared following previously reported procedures.[23] A prepared 1L bottle of the monomer was stored in a 3ºC refrigerator for approximately six months and exhibited no signs of decomposition.

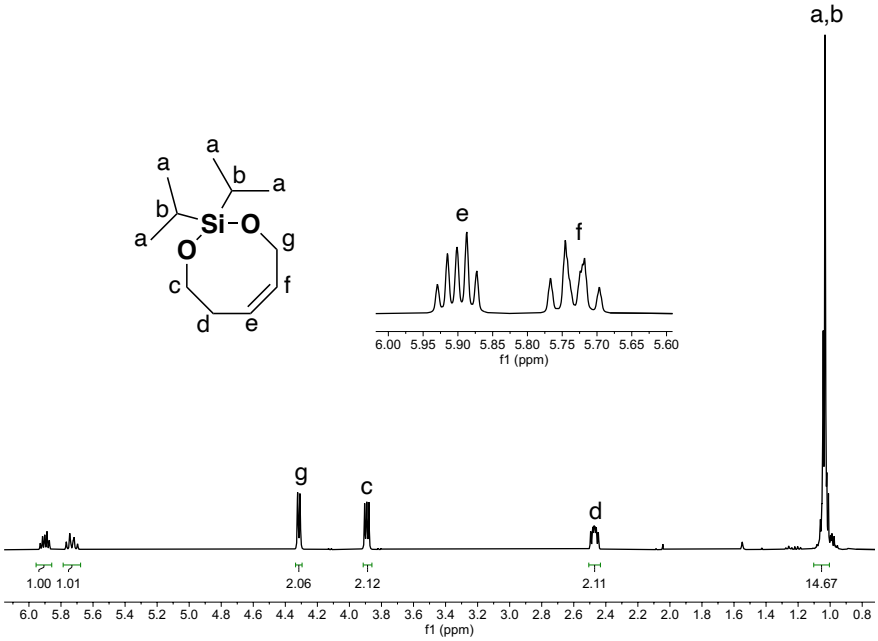

Figure S1. ^{1}H NMR spectrum (400 MHz, $CDCl_3$) of ^{i}PrSi8.

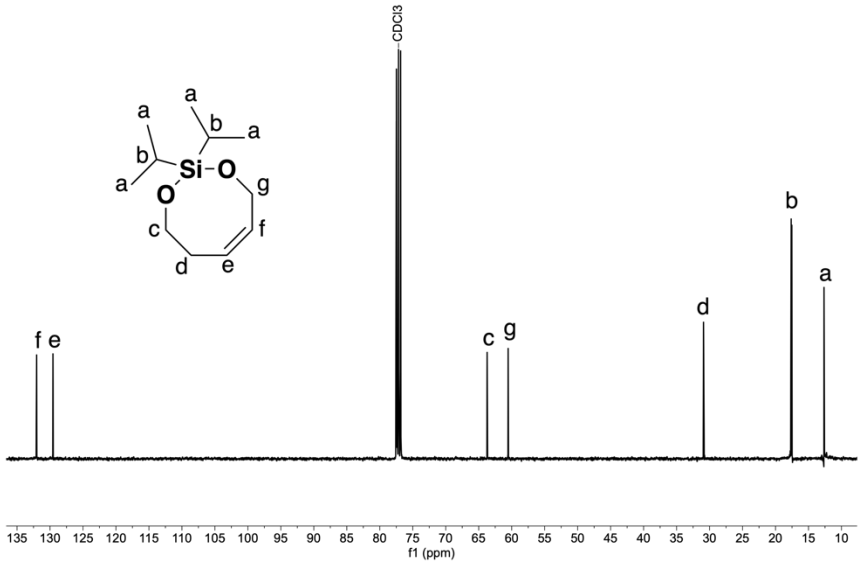

Figure S2. ^{13}C NMR spectrum (101 MHz, $CDCl_3$) of ^{i}PrSi8.

b. Homopolymerization of ^{i}PrSi8

The following is a specific example of the general procedure used to prepare poly(^{i}PrSi8) [Table 1, entry 12, $[M]_0$:[G3] = 500]. ^{i}PrSi8 (107 mg, 0.50 mmol) and anhydrous dioxane (815 µL) were added to a 40 mL scintillation vial equipped with a magnetic stir bar under nitrogen. A solution of G3 in dioxane (0.742 mg in 74.2 µL anhydrous dioxane, 0.001 mmol) was added and the mixture was stirred for two hours. An excess of ethyl vinyl ether was added to quench the reaction and was stirred for 15 min.

The polymerization solution was concentrated under vacuum to remove residual ethyl vinyl ether. The crude polymer was dissolved in ~10 mL toluene and added dropwise to a 10-fold excess of rapidly stirring MeOH, which was submerged in an ice bath. The precipitate was a gummy oil, which was collected and then this procedure was repeated twice more. To avoid excessive mechanical losses, especially on a small scale, pentane was used to quantitatively recombine the precipitated solid before each subsequent precipitation. After the final precipitation, residual solvents were removed from the sample under high vacuum until the mass remained constant.

Monomer conversions were calculated with ^{1}H NMR spectra by integrating the methine regions of the polymers and monomers against a 1,3,5-trimethoxybenzene internal standard. Conversion by ^{1}H NMR spectroscopy of the crude mixture was 96.1%, and gravimetric yield after precipitation was 89%. M_n of the precipitated polymer was found to be 159 kDa by SEC with a dispersity of 1.76. Cyclic oligomer content was calculated by following adaptations of previously reported procedures.[22]

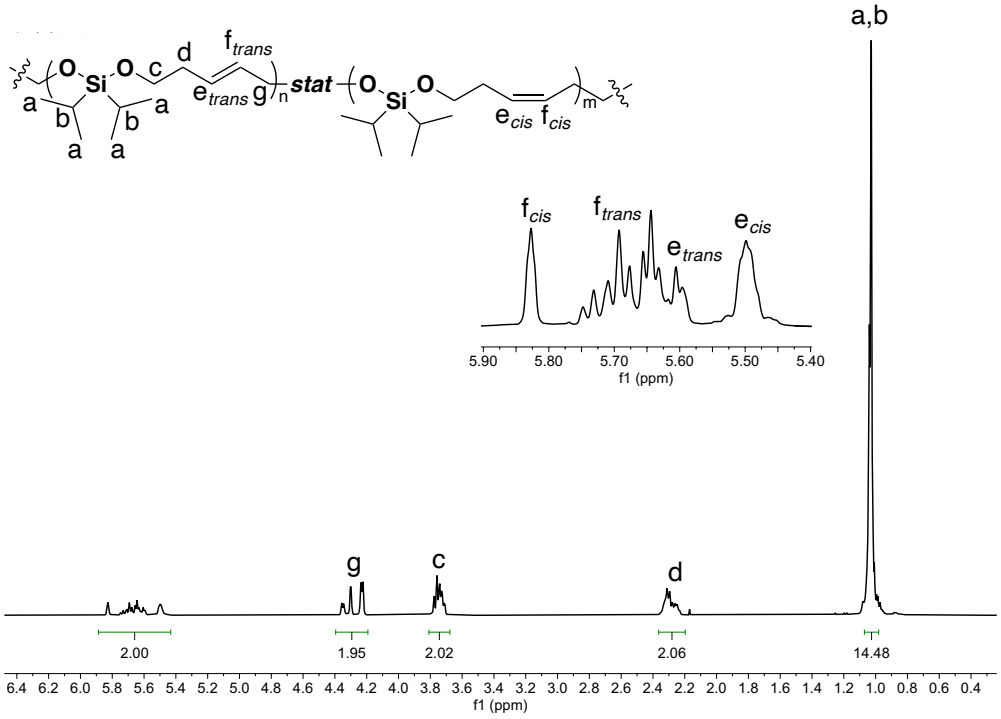

Figure S3. ^{1}H NMR spectra (400 MHz, $CDCl_3$) of poly(^{i}PrSi8).

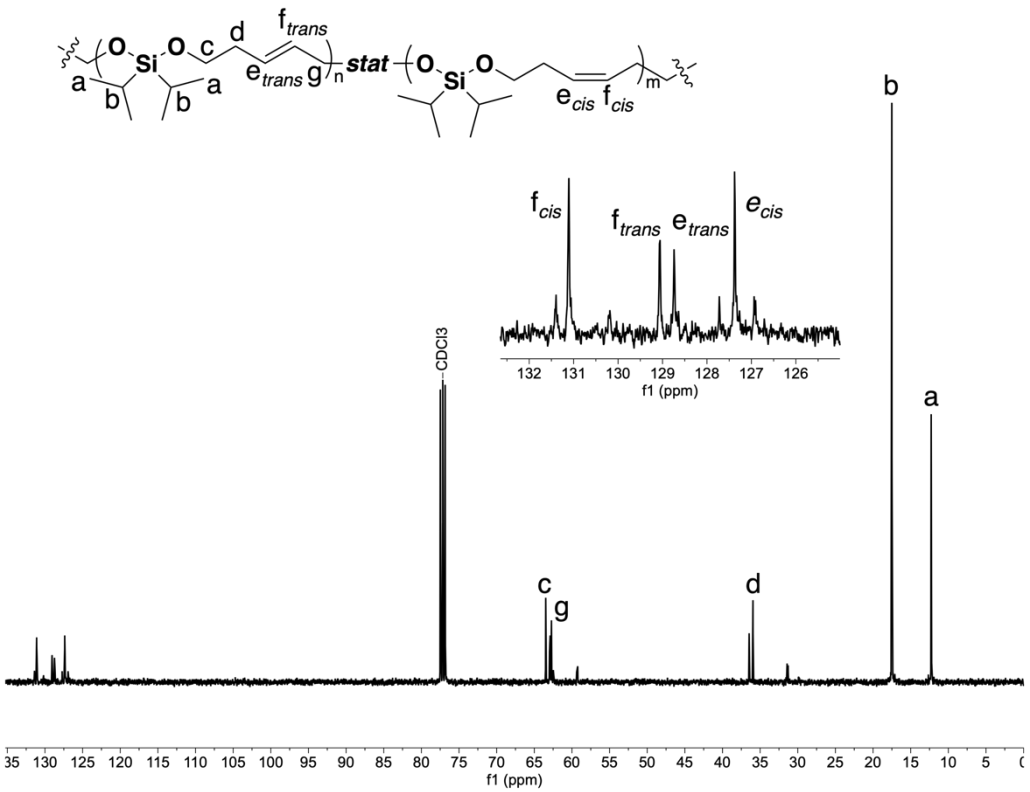

Figure S4. ^{13}C NMR spectra (101 MHz, $CDCl_3$) of poly(*i*PrSi8).

POLYMER DECONSTRUTION AND DEPOLYMERIZATION

a. G3-mediated depolymerization of poly(*i*PrSi8)

*i*PrSi8 (107 mg, 0.50 mmol) and anhydrous dioxane (815 µL) were added to a 40 mL scintillation vial equipped with a magnetic stir bar under nitrogen. A solution of G3 in dioxane (0.742 mg in 74.2 µL anhydrous dioxane, 0.001 mmol) was added and the mixture was stirred for two hours. 50 µL of the reaction was immediately quenched with excess ethyl vinyl ether. 50 µL each were transferred to vials prepared with 0.036 mg (5 x 10^{-6} mmol), 0.36 mg (5 x 10^{-4} mmol), and 3.6 mg (0.005 mmol) additional G3 under nitrogen. After an additional 2 h stirring, each was quenched with excess ethyl vinyl ether, concentrated under vacuum to remove residual ethyl vinyl ether, and analyzed by GPC and ^{1}H NMR without further purification.

*i*PrSi8 (150 mg, 0.70 mmol) and anhydrous dioxane (155 µL) were added to a 10 mL scintillation vial equipped with a magnetic stir bar under nitrogen. A solution of G3 in dioxane (0.52 mg mg in 14.0 µL anhydrous dioxane, 0.0007 mmol) was added and the mixture was stirred for two hours. Half of the reaction was immediately quenched with excess ethyl vinyl ether. The remaining half was transferred to a vial prepared with 2.6 mg (0.0035 mmol) additional G3 under nitrogen. After an additional 2 h stirring, the reaction was quenched with excess ethyl vinyl ether. Both solutions were concentrated under vacuum to remove residual ethyl vinyl ether and analyzed by GPC.

b. Fluoride-mediated deconstruction of poly(*i*PrSi8)

The polymerization solution was concentrated under vacuum to remove residual ethyl vinyl ether. The solutions were treated with an excess of 0.2 TBAF in THF and the mixture was stirred for 30 minutes. Excess AmberChrom® 50WX2 was added and the mixture was allowed to sit for 5 min. Finally, the mixture was extracted with DCM, filtered with a 0.2 μm nylon filter, concentrated to remove volatile difluorodiisopropylsilane, and analyzed by GPC.

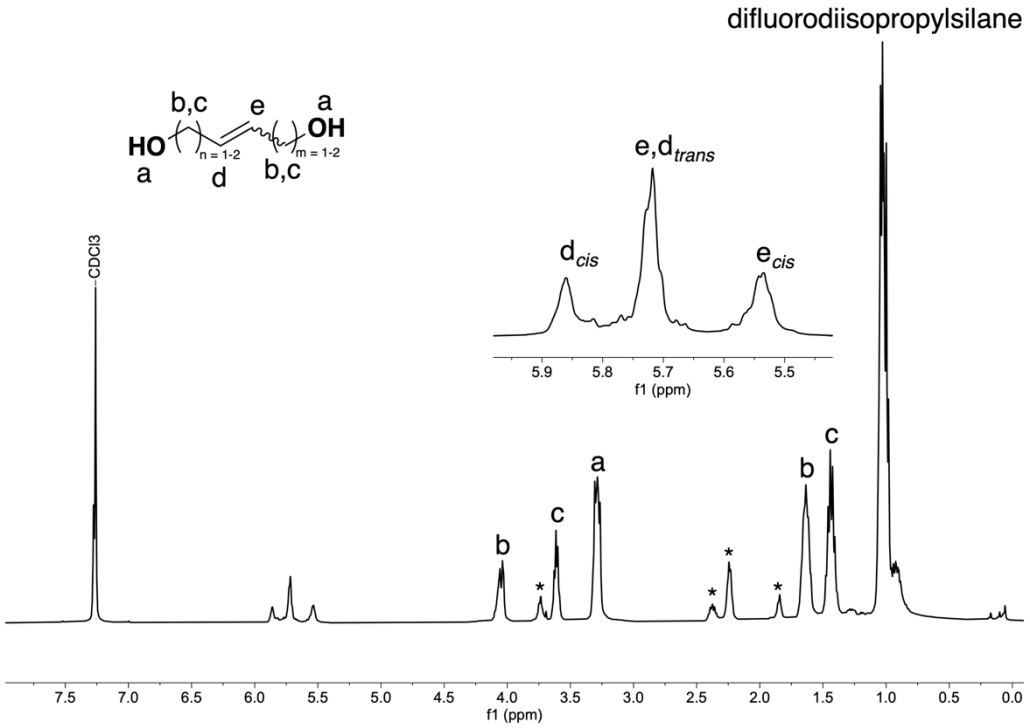

Figure S5. ^{1}H NMR spectrum (400 MHz, $CDCl_3$) of fluoride-treated poly(*i*PrSi8).

c. Acid-mediated deconstruction of poly(*i*PrSi8)

The polymerization solution was concentrated under vacuum to remove residual ethyl vinyl ether. The solutions were treated with an excess of 0.5 M HCl in dioxane and the mixture was stirred for 30 minutes. Excess sodium sulfate was added and the mixture was allowed to sit for 5 min. Finally, the mixture was extracted with DCM, filtered with a 0.2 μm nylon filter, concentrated to remove volatile diisopropylsilanediol, and analyzed by GPC.

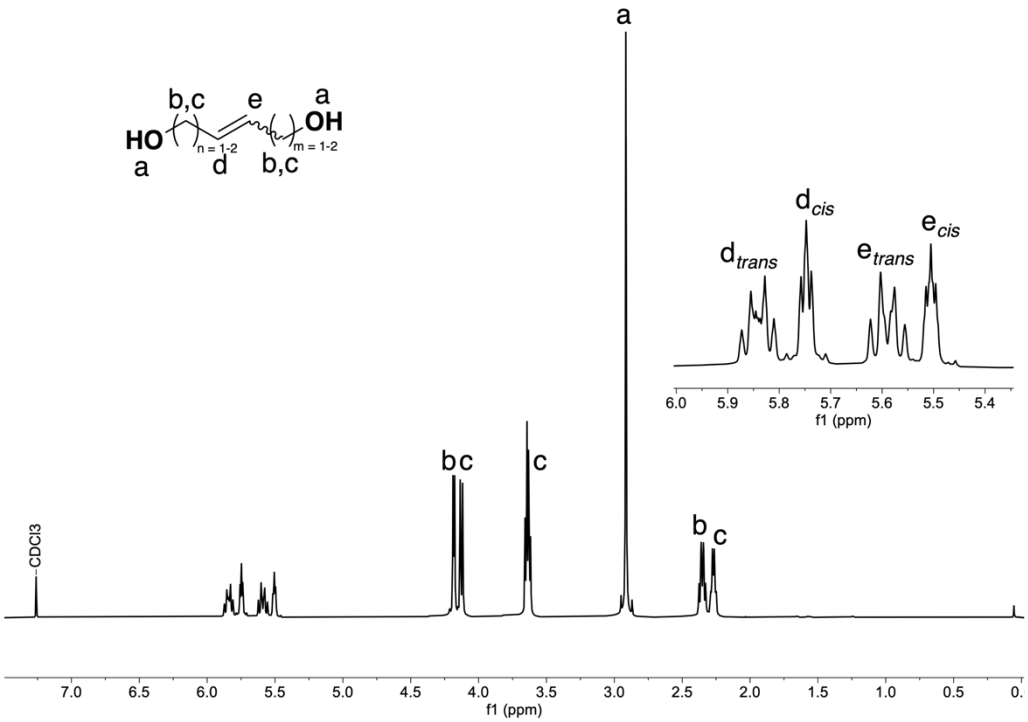

Figure S6. ^{1}H NMR spectrum (400 MHz, $CDCl_3$) of acid-treated poly(*i*PrSi8).

REGIOSELECTIVITY EXPERIMENTS

a. Acetylation of ene-diols

A 40 mL scintillation vial equipped with a stir bar was charged with the fluoride-deconstructed ene diol mixture (0.35 g, 3.62 mmol), 4-dimethylaminopyridine (22 mg, 0.181 mmol), and triethylamine (1.47 g, 14.5 mmol). The reaction was cooled in an ice bath under N_2 and acetic anhydride (1.11 g, 10.9 mmol) was added dropwise over 15 min. The reaction was allowed to warm to room temperature overnight. The brown mixture was washed with HCl (pH 3, 2 x 20 mL x 2), $NaHCO_3$ (2 x 20 mL), and brine (20 mL). The organic layer was collected, dried over $NaSO_4$, and concentrated to yield a brown oil (>98% crude).

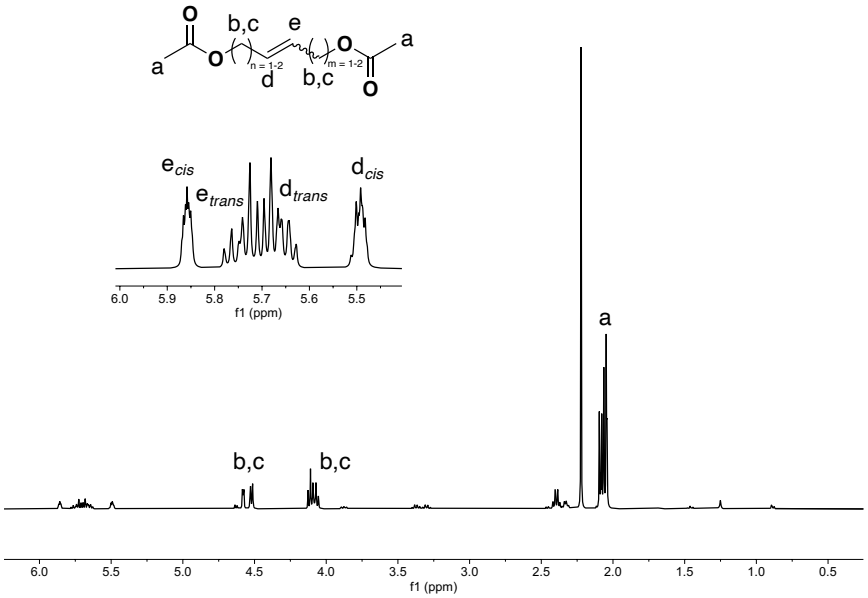

Figure S7. ^{1}H NMR spectrum (400 MHz, $CDCl_3$) of crude mixture of acteylated ene-diols.

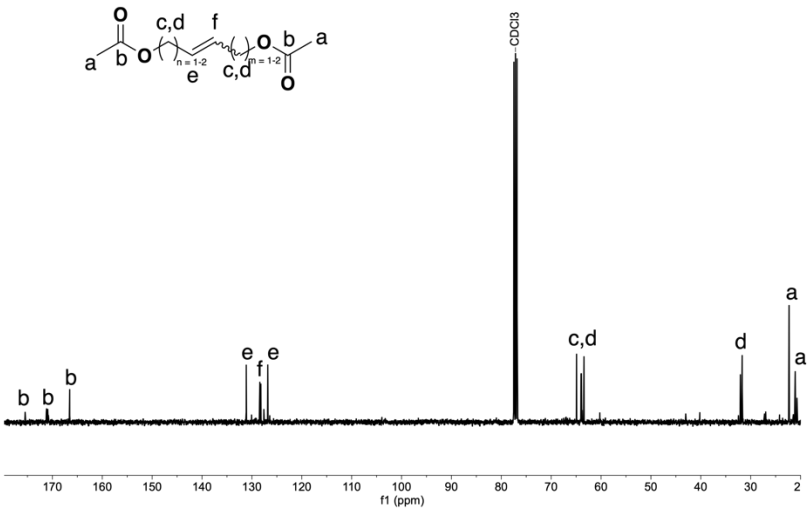

Figure S8. ^{13}C NMR spectrum (101 MHz, $CDCl_3$) of crude mixture of acetylated ene-diols.

b. Hydrogenation of acetylated ene-diols

Pd/C (5 mg, 0.05 mmol) was weighed into a 50 mL RBF equipped with a stir bar under N_2 and suspended in anhydrous THF (~5 mL). The acetylated ene-diol mixture (100 mg, 0.5 mmol) was added via microsyringe. The reaction was allowed to stir overnight under a balloon of H_2. The reaction was poured over a pad of celite, washed with ~30 mL DCM, concentrated to yield a brown oil (>98% crude).

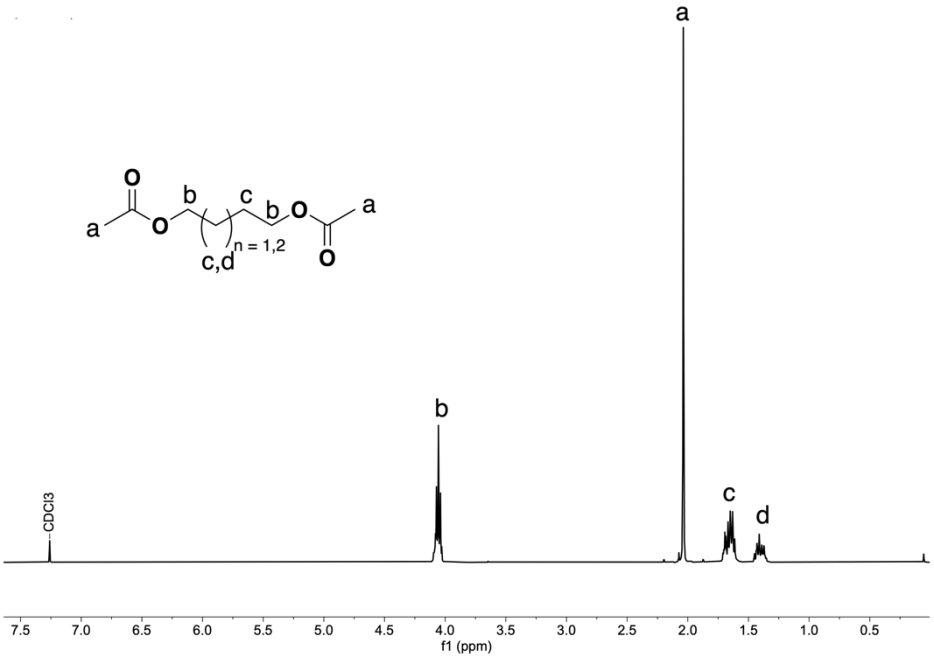

Figure S9. ^{1}H NMR spectrum (400 MHz, $CDCl_3$) of hydrogenated ene-diols.

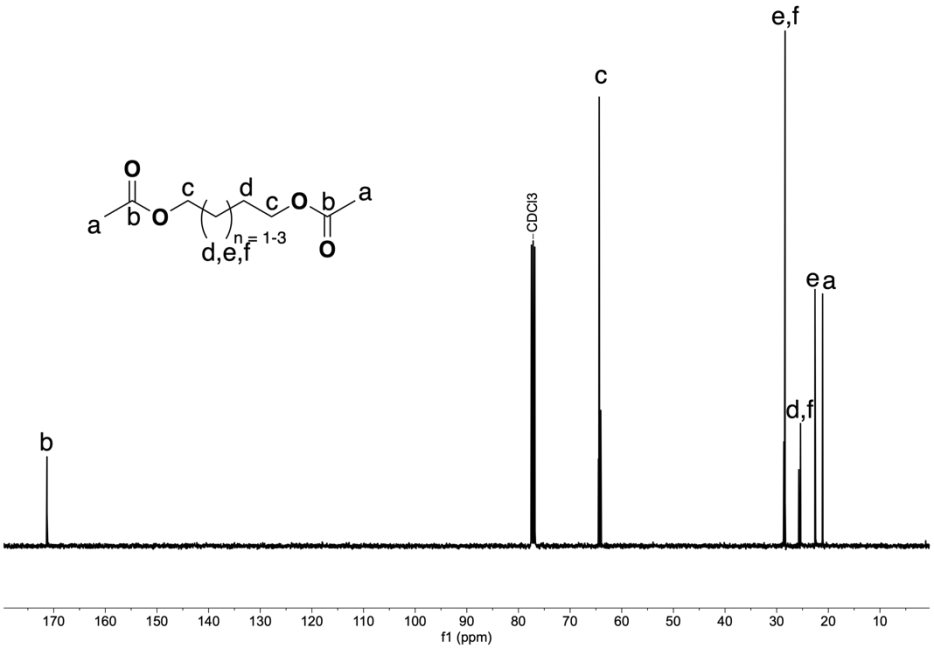

Figure S10. ^{13}C NMR spectrum (101 MHz, $CDCl_3$) of hydrogenated ene-diols.

c. GC-MS calibration and regiochemical analysis

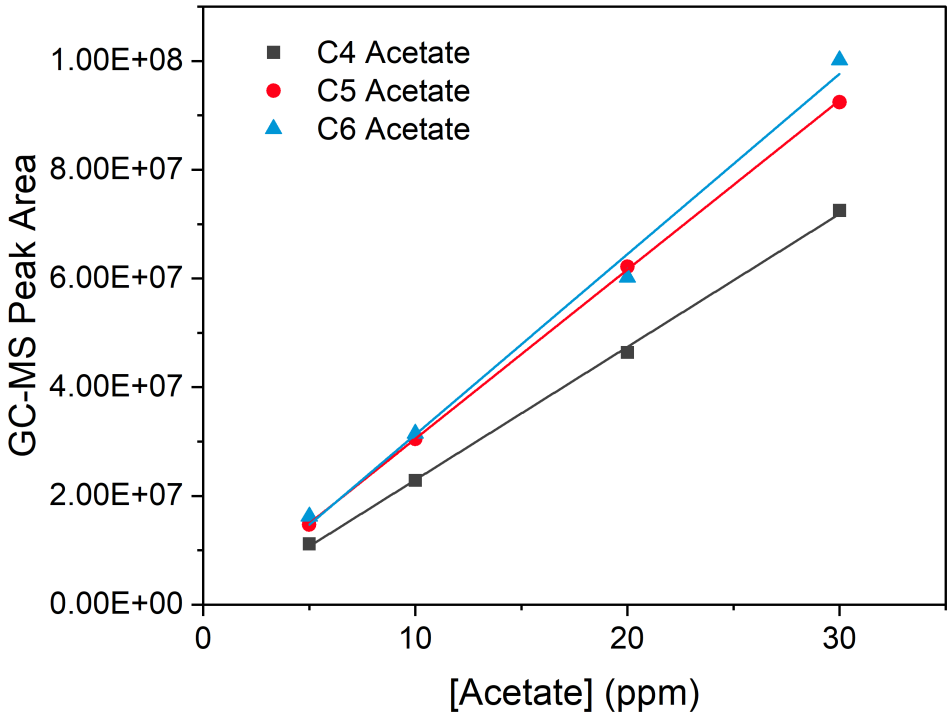

Figure S11. GC-MS calibration curves. C4 R^2=0.999, C5 R^2=0.999, C6 R^2=0.993.

Table S1. GC-MS data. The relative concentration of each sized acetate was found by normalizing the concentration of [C5] to 2.0.

entry	C4 Peak Area	[C4] (ppm)	[C4] relative	C5 Peak Area	[C5] relative	[C5] (ppm)	C6 Peak Area	[C6] (ppm)	[C6] (ppm)
1	10151965	4.8	0.9	32796863	2.0	10.7	21824231	1.3	7.2
2	17841951	7.9	0.9	57038321	2.0	18.5	36813535	1.3	11.2
3	26897400	11.6	0.8	90172306	2.0	29.2	60982700	1.3	19.0
4	22410887	9.8	0.8	75401222	2.0	24.4	46462559	1.2	14.6
5	28478833	12.3	0.8	90437707	2.0	29.3	60534800	1.3	18.8
Average			0.8		2.0			1.3	
Std Dev.			0.0386		–			0.0520	